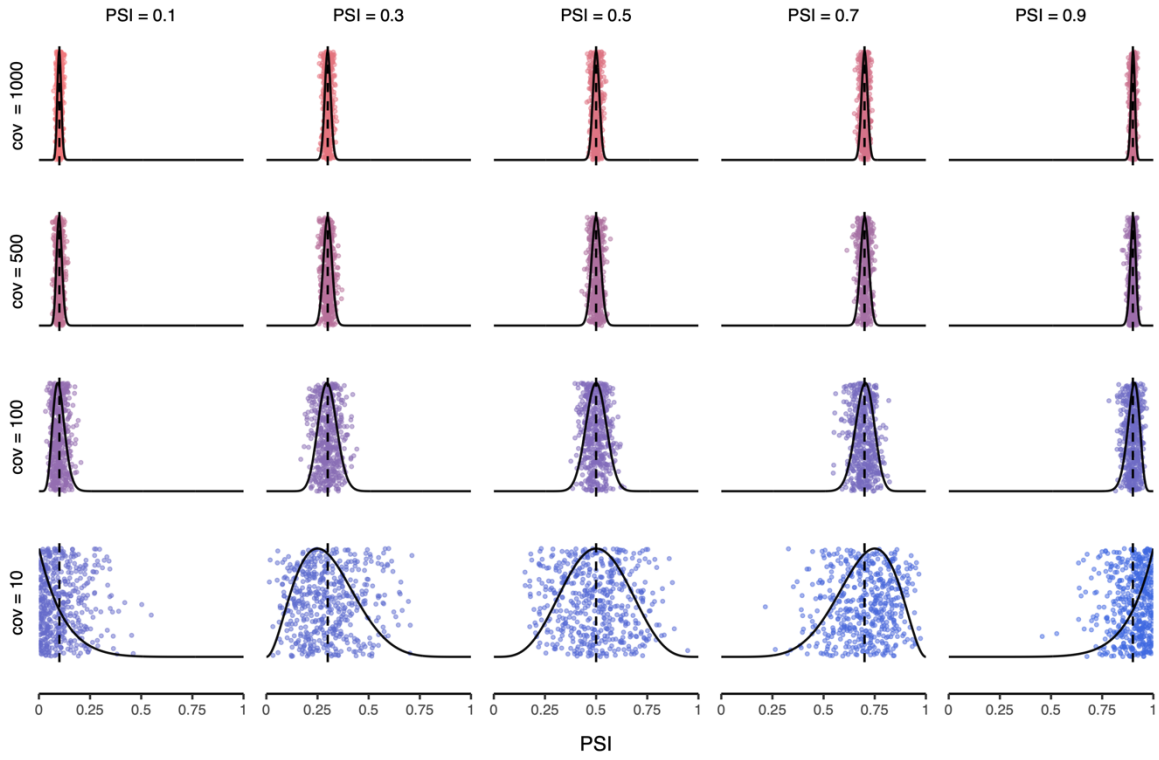

Supplemental Figure S1. Beta distributions model PSI levels and associated confidence. Density plots (black lines) illustrating the dispersion of 500 values randomly generated from beta distributions (coloured vertically "jittered" points) modelling different PSI levels (columns) supported by different levels of coverage (cov) in junction read counts (rows).

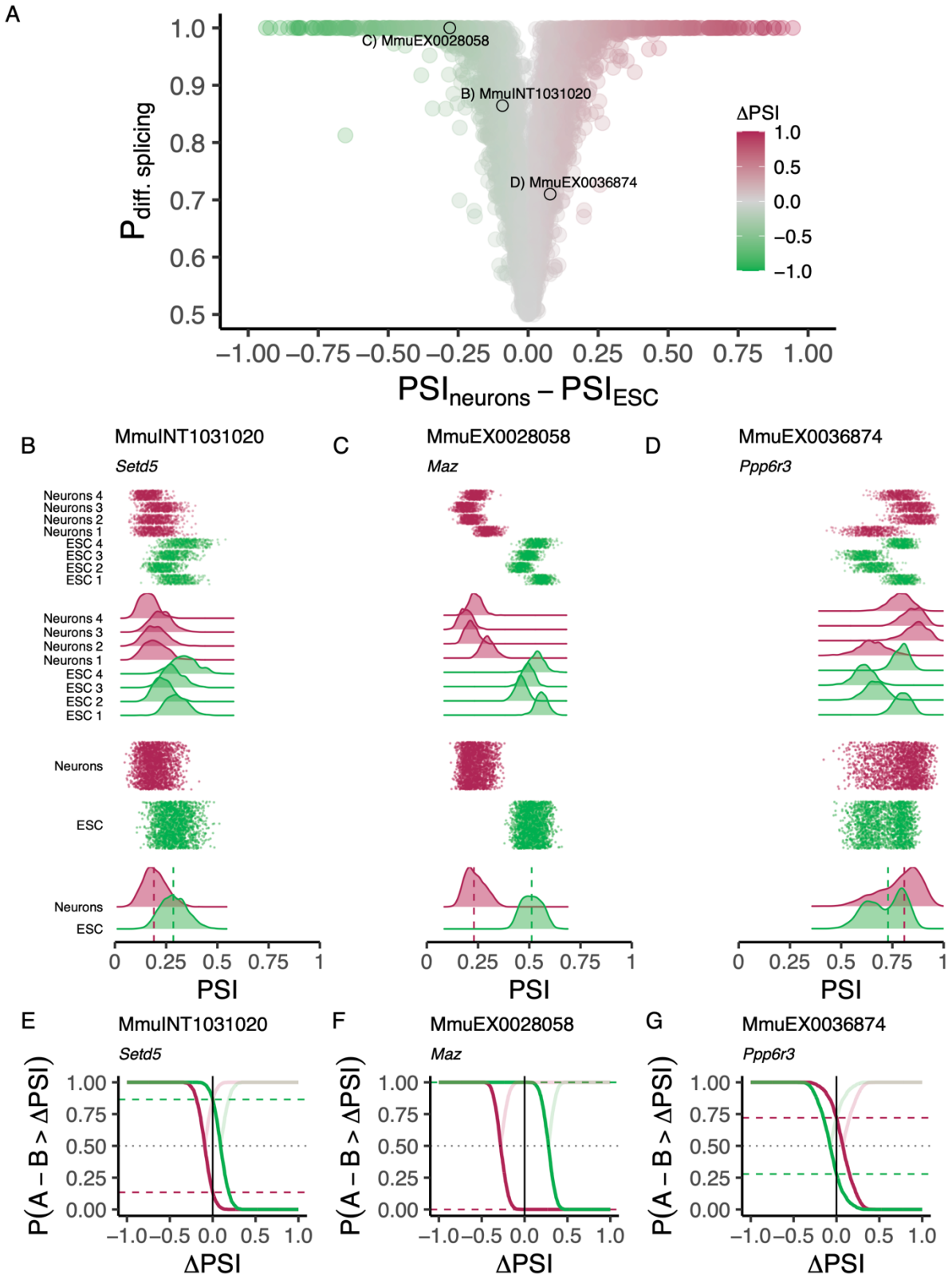

Supplemental Figure S2. Estimating the probability of differential alternative splicing. (**A**) Volcano plot illustrating the effect size (ΔPSI) as the difference between the median group PSIs and their significance assessed by the estimated probability of differential AS, based on the proportion of differences between ESC and Neurons beta distribution randomly emitted values that are > 0 (P_{diff}). Events are coloured by the ΔPSI calculated between neuronal and ESC samples. Marked events are

illustrative of different scenarios of estimated P_{diff}. (**B** to **D**) Beta distributions (vertical "jitter" and density plots of the emitted values) per sample (top) and per phenotypic group (bottom) and (**E** to **G**) cumulative line plots of the probability that the differences between values in sample groups A and B under comparison (A = ESC and B = neurons for the green line, with P(A – B > ΔPSI) reflecting P (ESC – neurons > ΔPSI); same for the red line, with A = neurons and B = ESC, to illustrate the symmetry in P_{diff} calculation) are greater than a given value of ΔPSI for selected events illustrative of different scenarios of estimated P_{diff}: (**B,E**) MmuINT1031020 (gene *Setd5,* chr6:113109991-113110373), (**C,F**) MmuEX0028058 (gene *Maz*, chr7:127023482-127023706), (**D,G**) MmuEX0036874 (gene *Ppp6r3*, chr19:3544108-3544255). ESC: embryonic stem cells.

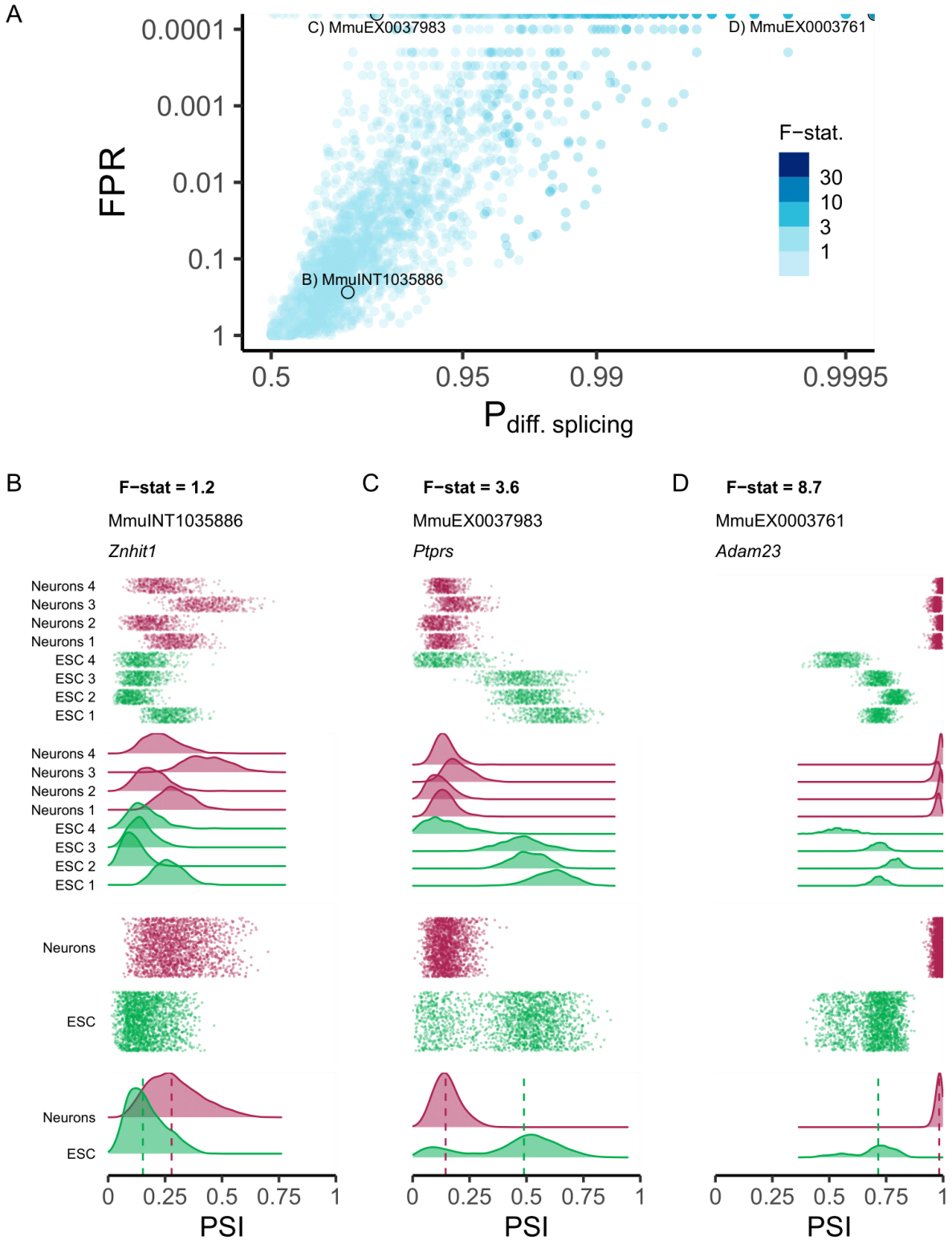

Supplemental Figure S3. Estimating an F-statistic for differential alternative splicing. (**A**) Scatterplot comparing `betAS` metrics to estimate the significance of AS differences: false positive rate (FPR) and the probability of differential splicing, $P_{diff\ splicing}$. Events are coloured by the F-statistic, i.e., the ratio of between- to within-group PSI variations. Marked events are illustrative of different scenarios of estimated P_{diff}, FPR and F-statistic. Y-axis scales are log-transformed to facilitate visualisation. (**B** to **D**) Beta distributions (vertical jitter and density plots of the emitted values) per sample (top) and per group (bottom) of selected events illustrative of different scenarios of estimated F-statistic: (**B**)

MmuINT1035886 (gene *Znhit1,* chr5:136985050-136987488), (**C**) MmuEX0037983 (gene *Ptprs*, chr17:56428852-56429157), (**D**) MmuEX0003761 (gene *Adam23*, chr1:63585365-63585455). ESC: embryonic stem cells.

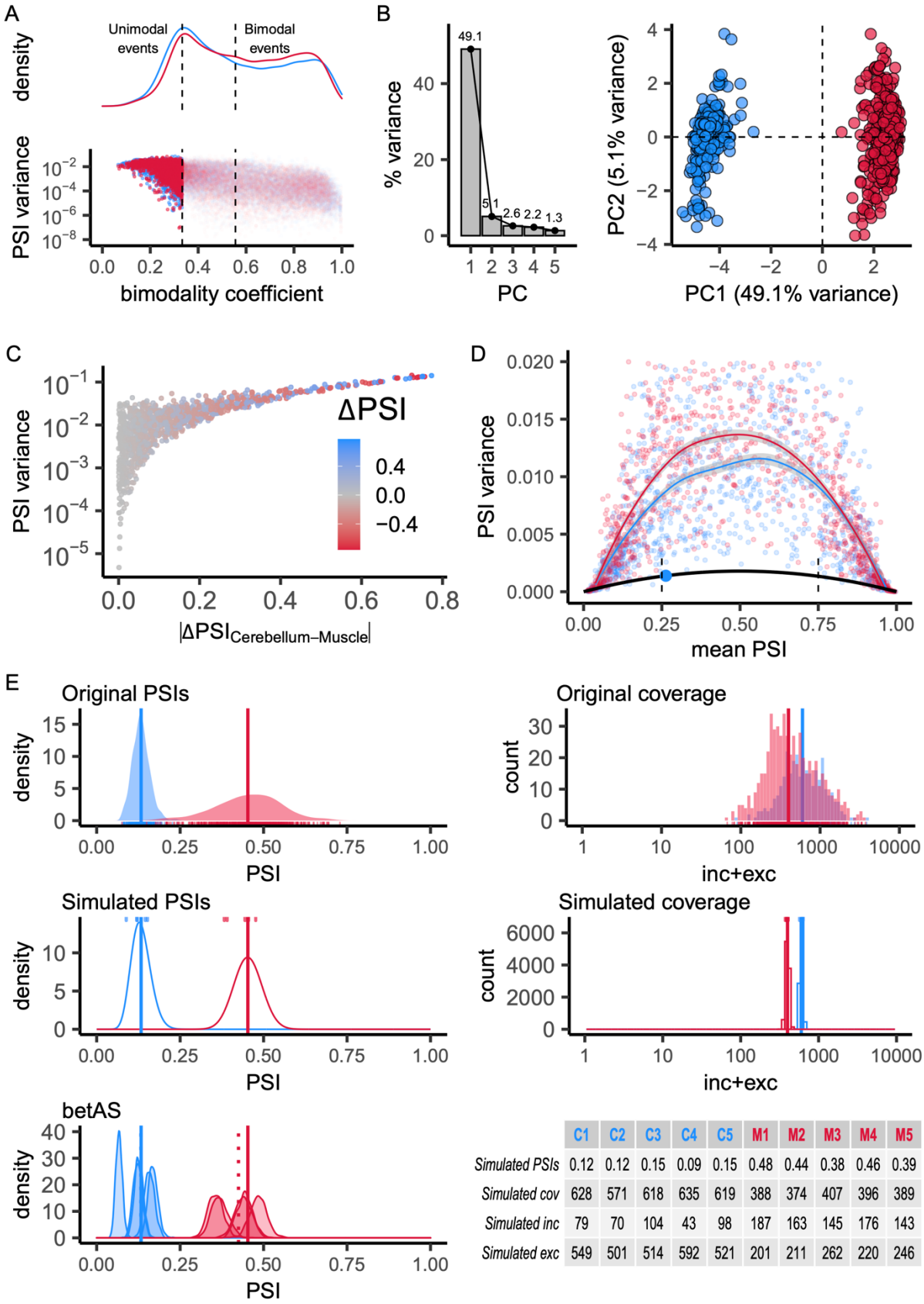

	C1	C2	C3	C4	C5	M1	M2	M3	M4	M5
Simulated PSIs	0.12	0.12	0.15	0.09	0.15	0.48	0.44	0.38	0.46	0.39
Simulated cov	628	571	618	635	619	388	374	407	396	389
Simulated inc	79	70	104	43	98	187	163	145	176	143
Simulated exc	549	501	514	592	521	201	211	262	220	246

Supplemental Figure S4. Simulation of empirically-inspired junction read counts. (**A**) Bottom: scatterplot of log-transformed PSI variance against the bimodality coefficient for considered events in muscle (red) and cerebellum (blue). Top: density plot of the bimodality coefficient for muscle and cerebellum, illustrative of unimodal and bimodal subpopulations. Vertical dashed lines indicate

bimodality coefficients cut-offs: events were considered unimodal if bimodality coefficient < 3/9 and bimodal if bimodality coefficient > 5/9. (**B** to **D**) Subset of unimodal events only. (**B**) Principal component analysis (PCA) performed on the centred, unscaled original PSI values. Left: Percentage of variance explained by each of the five first principal components (PC). Right: Scatterplot of samples' loadings on PCs 1 and 2. (**C**) Scatterplot of log-transformed PSI variance against the ΔPSI between cerebellum's and muscle's PSI_{REF}. (**D**) Scatterplot of PSI variance to PSI mean relationship for a subset of low variance events (PSI variance < 0.02), allowing the empirical determination of the lowest PSI variance (the least biological noise) within considered PSI values (point highlighted in blue) and the respective PSI variance/mean relationship (black curve). Vertical dashed lines indicate the mean PSI range considered to identify a subset of representative low variance events. (**E**) Illustrative example of the procedure to simulate RNA-seq junction read counts based on simulated PSIs and coverage on which `betAS` is applied. "Original PSIs": density and rug plot showing the original distribution of PSI values for all samples; vertical lines indicate PSI_{REF} values for muscle and cerebellum. "Original coverage": histogram and rug plot showing the original distribution of coverage values for all samples; vertical lines indicate cov_{REF} values for muscle and cerebellum. "Simulated PSIs": density plot showing the beta distribution from which low variance PSI values around the mean of PSI_{REF} (vertical lines) are simulated (top rug plot). "Simulated coverage": histogram showing the Poisson distribution from which coverage values around cov_{REF} (vertical lines) are simulated (top rug plot). "betAS": density plots representing PSI estimation as done in `betAS`, with values randomly emitted from a beta distribution with the shape associated with the simulated junction read counts per sample. Table compiling simulated PSI, coverage and junction read count (inc and exc) values for the 5 simulated cerebellum (C1 to C5) and muscle (M1 to M5) replicates. Solid vertical lines indicate PSI_{REF} values for muscle and cerebellum, while dashed vertical lines indicate the median PSI values estimated by `betAS` for muscle and cerebellum.

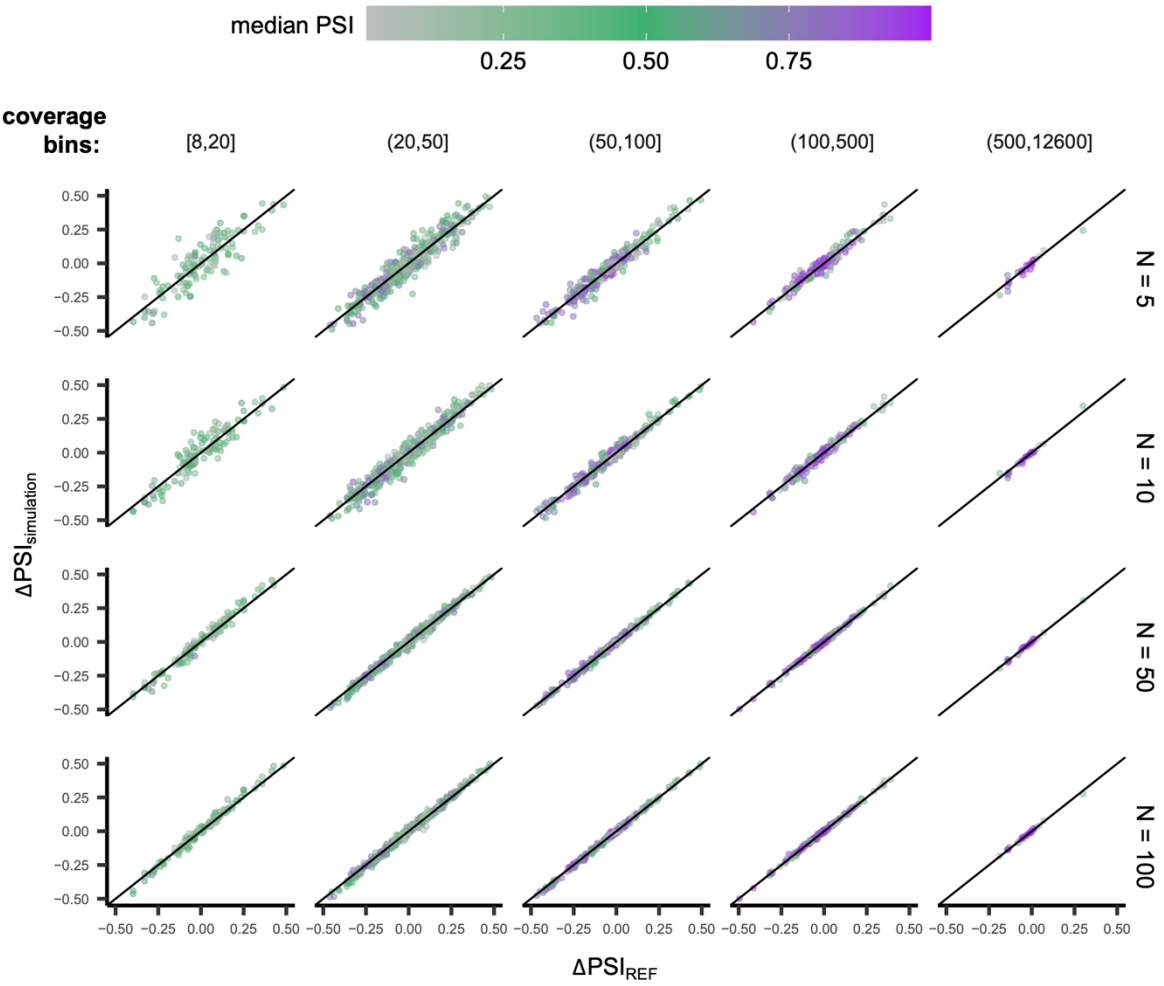

Supplemental Figure S5. betAS accuracy in measuring PSI differences from simulated read counts. Scatterplots comparing the ΔPSI obtained by applying betAS to the simulated junction read counts, $\Delta PSI_{simulation}$, with the reference ΔPSI_{REF} for the subset of unimodal events considered, for different numbers of replicates (N, rows) and coverage ranges (in junction read counts, columns).

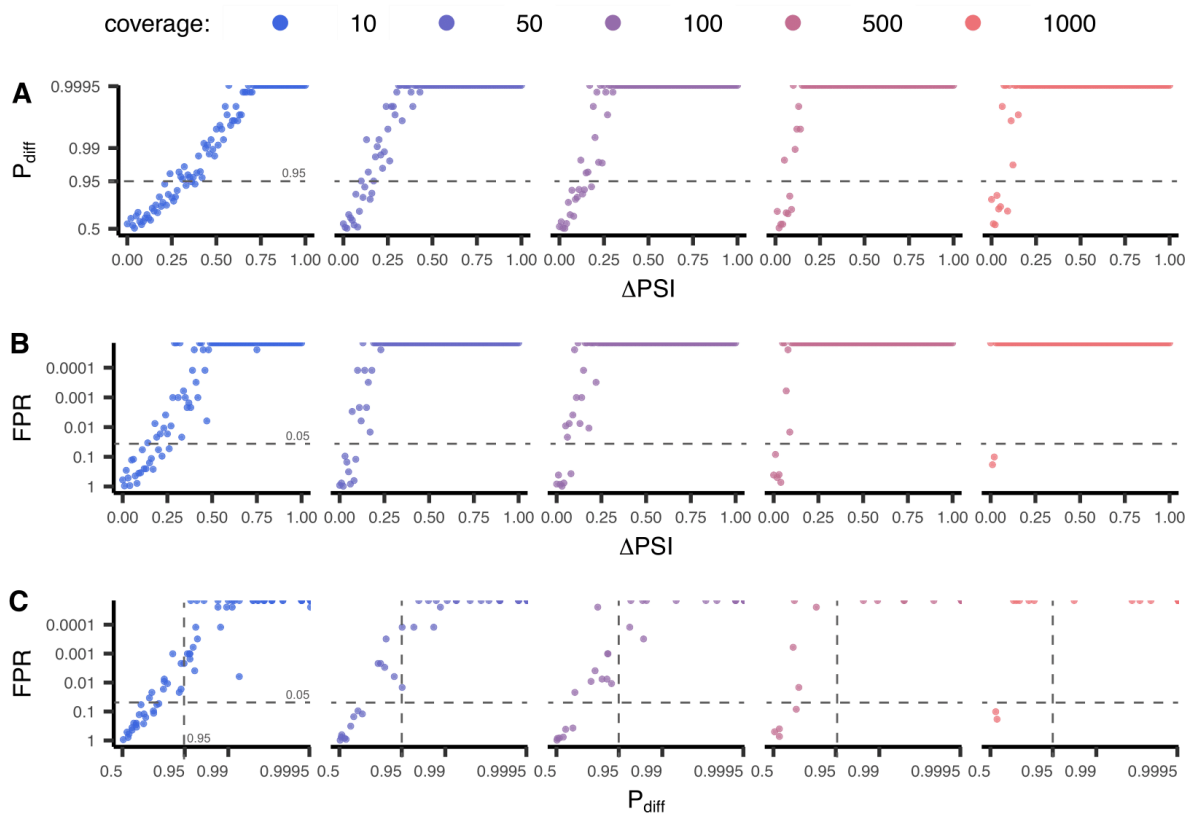

Supplemental Figure S6. The impact of simulated cases of effect size (ΔPSI) and coverage pairs in P_{diff} (**A**) and FPR (**B**). P_{diff} and FPR values (directly compared in **C**) obtained for the differential splicing analysis comparing three biological replicate PSI values. Simulated PSI values were obtained considering ΔPSI ranging from 0 to 1 in intervals of 0.01 and coverage of 10, 50, 100, 500 or 1000 read counts. For each ΔPSI and coverage pair, two random PSI values were obtained with a difference of ΔPSI; for each of these PSI values, biological PSI triplicates were obtained by emitting 3 values from a beta distribution with parameters such that $\alpha + \beta = 138.5042$ (see Supplemental Methods).

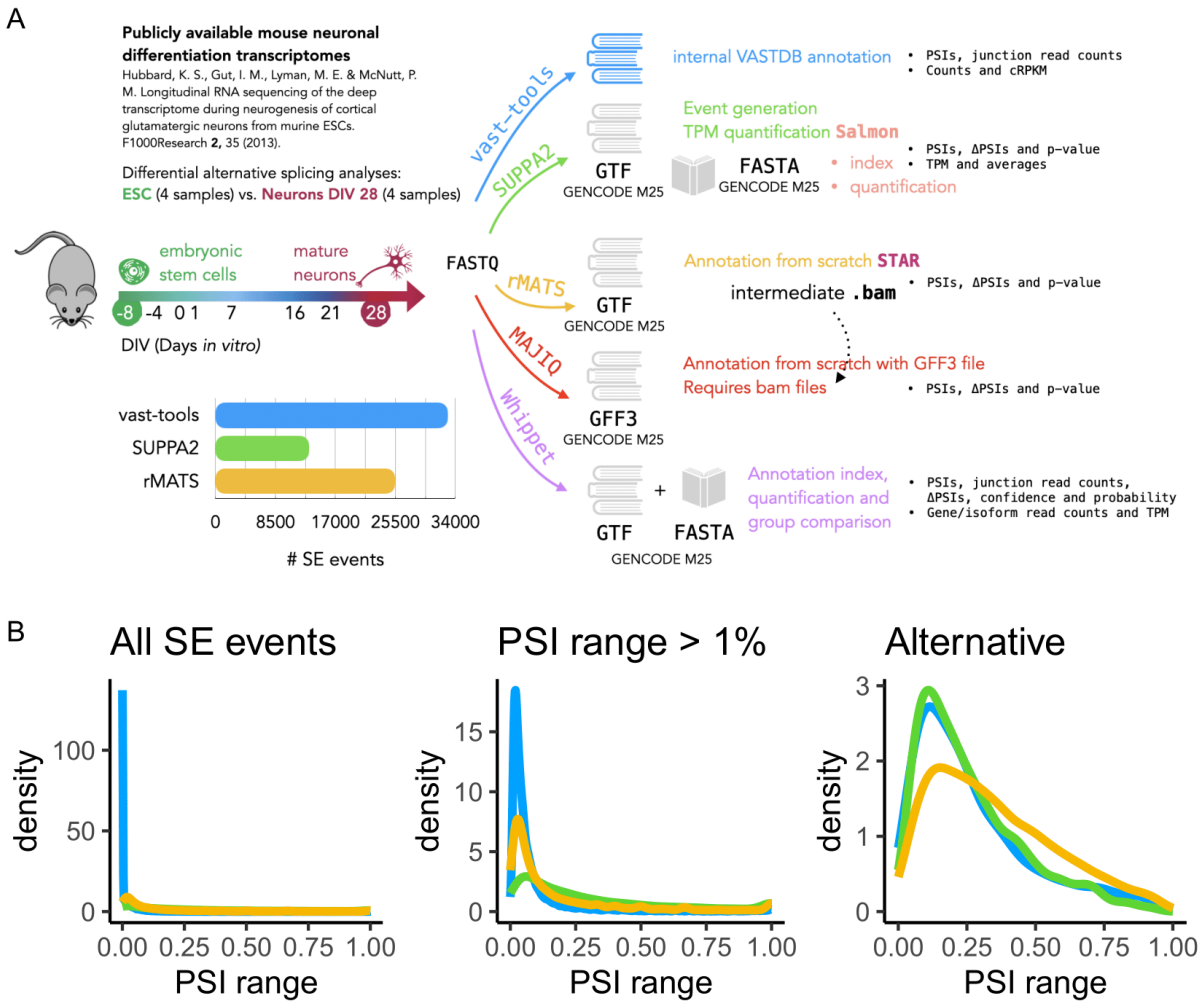

Supplemental Figure S7. Comparison of differential alternative splicing analysis tools. (**A**) Explanatory diagram of the approach to obtain read counts and differential AS quantification metrics for each studied tool. (**B**) Density plots of the distribution of PSI for all exon skipping (SE) events considered (left), those with a PSI range (maximum to minimum PSI) > 1% (middle) and alternative events (0 < PSI < 1, right) for `vast-tools` (blue), SUPPA (green) and rMATS (yellow).

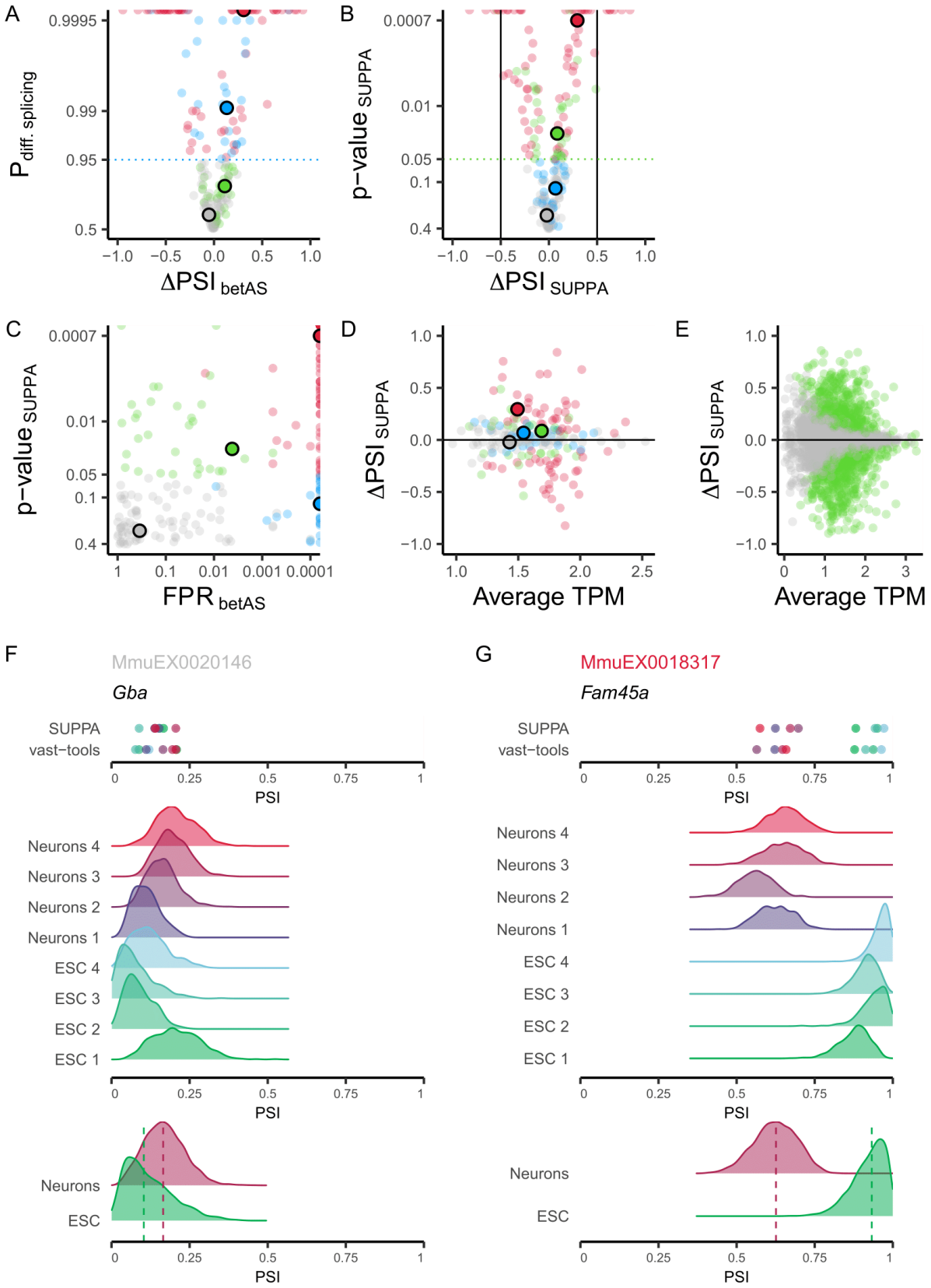

Supplemental Figure S8. Comparison of differential AS between betAS and SUPPA. (**A**) betAS' volcano plot of differential AS (each AS event represented by a dot) illustrating the effect sizes (ΔPSI_{betAS}) as the differences between the median group PSIs and their significance assessed by the estimated probability of differential AS, based on the proportion of differences between beta distributed randomly emitted values per sample group that are > 0 ($P_{diff.\ splicing}$). The blue dashed

horizontal line indicates the considered cut-off of P_{diff} = 0.95. (**B**) SUPPA's volcano plot of differential AS illustrating the effect sizes (ΔPSI_{SUPPA}) and their significance assessed by SUPPA's p-value. The green dashed horizontal line indicates the considered cut-off of p-value = 0.05. (**C**) Scatterplot comparing betAS' and SUPPA's significance metrics for differential AS: betAS' false positive rate (FPR) and SUPPA's p-value. Points are coloured based on the differential AS calls by both tools as in Fig. 4: events considered differentially spliced by both betAS and SUPPA (red), by betAS (blue) or SUPPA (green) alone or by none of the tools (grey). (**D** and **E**) Scatterplots comparing ΔPSI_{SUPPA} with the respective transcript's average expression in transcripts per million (TPM) for the subset of events analysed between betAS and SUPPA (**D**) and for all SUPPA events (**E**). (**E**) events highlighted in green are those called differentially spliced by SUPPA (p-value < 0.05). (**F** and **G**) SUPPA and vast-tools' PSIs (top) and densities of emitted beta distributed values for individual samples (middle) and their merging per sample group (bottom, with dashed lines signing median values) for selected events illustrative of different combinations of effect size and significance of AS differences, identified by vast-tools' IDs (VAST-DB annotation for the mouse mm10 genome assembly): (**F**) MmuEX0020146 (gene *Gba,* chr3:89203192-89203360), (**G**) MmuEX0018317 (gene *Fam45a*, chr19:60817531-60817610). ESC: embryonic stem cells.

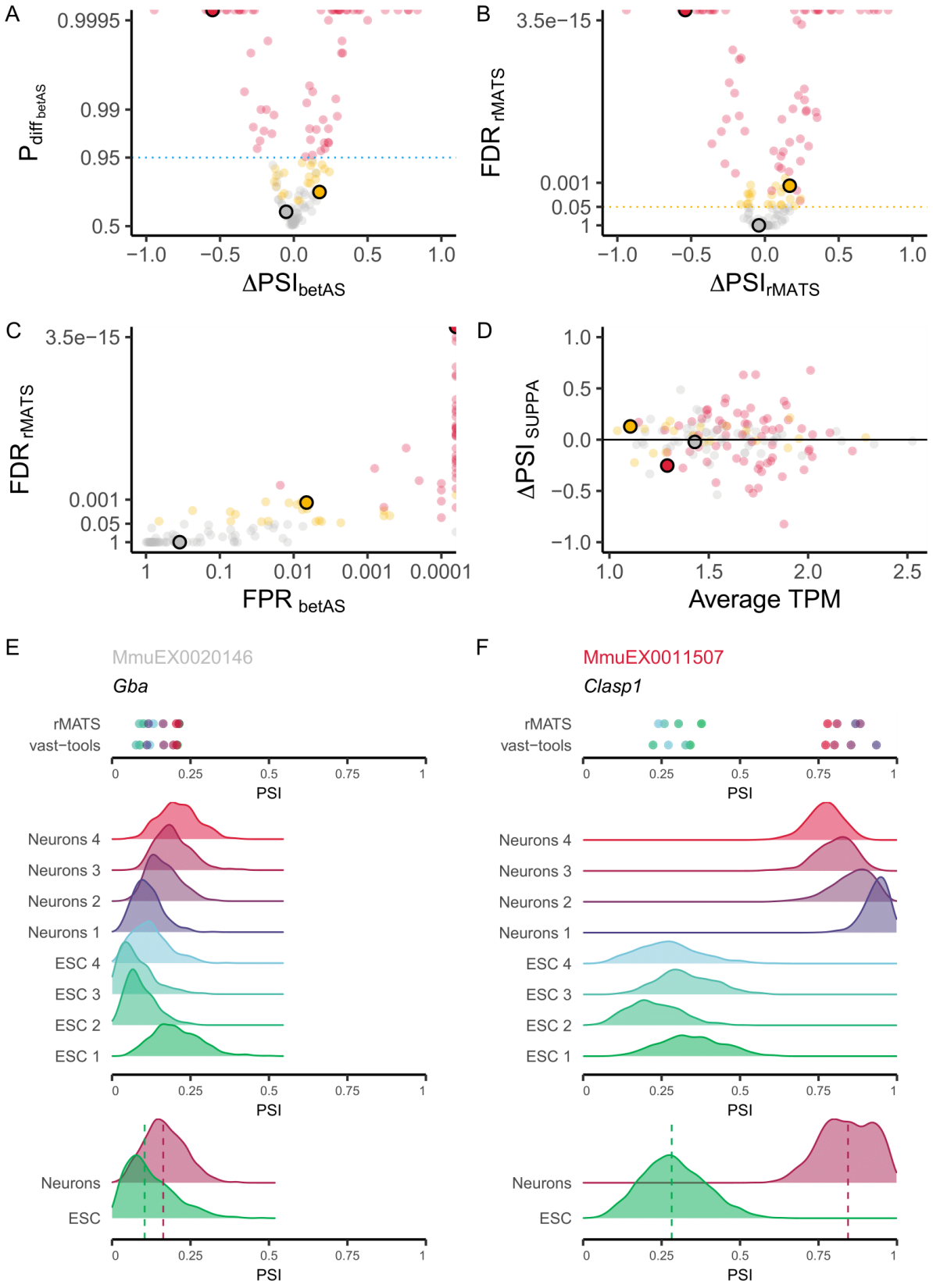

Supplemental Figure S9. Comparison of differential AS between betAS and rMATS. (**A**) betAS' volcano plot of differential AS (each AS event represented by a dot) illustrating the effect sizes (ΔPSI_{betAS}) as the differences between the median group PSIs and their significance assessed by the estimated probability of differential AS, based on the proportion of differences between beta

distributed randomly emitted values per group that are > 0 ($P_{diff\ betAS}$). The blue dashed horizontal line indicates the considered cut-off of P_{diff} = 0.95. (**B**) rMATS's volcano plot of differential AS illustrating the effect sizes (ΔPSI_{rMATS}) and their significance assessed by rMATS's FDR. The yellow dashed horizontal line indicates the considered cut-off of FDR = 0.05. (**C**) Scatterplot comparing betAS' and rMATS's significance metrics for differential AS: betAS' false positive rate (FPR) and rMATS' FDR. Points are coloured based on the differential AS calls by both tools as in Fig. 4: events considered differentially spliced by both betAS and rMATS (red), by betAS (blue) or rMATS (yellow) alone or by none of the tools (grey). (**D**) Scatterplots comparing ΔPSI_{SUPPA} with the respective transcript's average expression in transcripts per million (TPM) for the subset of events analysed between betAS, rMATS and SUPPA. (**E** and **F**) rMATS and vast-tools' PSIs (top) and densities of emitted beta distributed values for individual samples (middle) and their merging per sample group (bottom, with dashed lines signing median values) for selected events illustrative of different combinations of effect size and significance of AS differences, identified by vast-tools' IDs (VAST-DB annotation for the mouse mm10 genome assembly): (**E**) MmuEX0020146 (gene *Gba,* chr3:89203192-89203360), (**F**) MmuEX0011507 (gene *Clasp1*, chr1:118541675-118541698). ESC: embryonic stem cells.

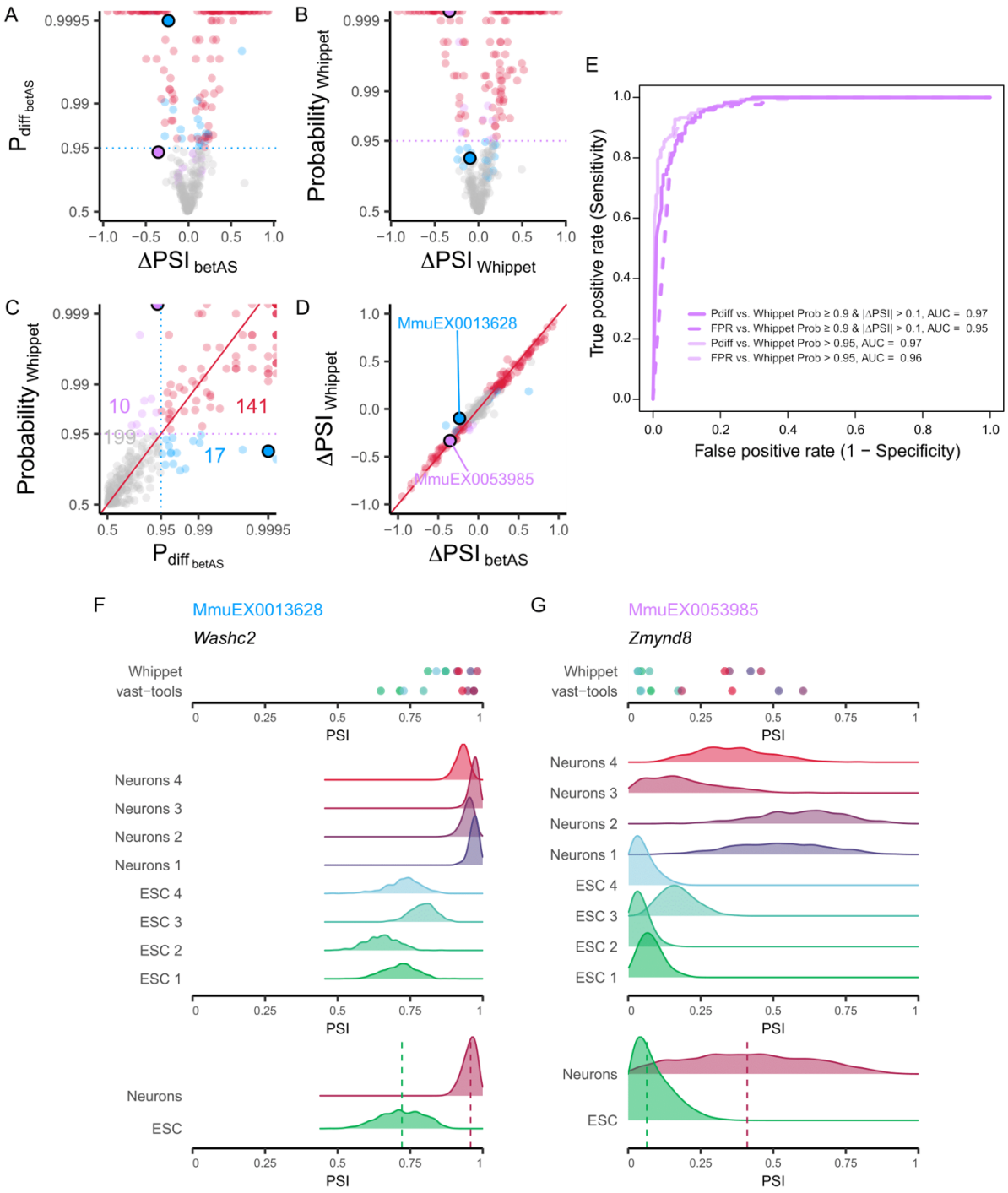

Supplemental Figure S10. Comparison of differential AS between `betAS` and `Whippet`. (**A**) `betAS`' volcano plot of differential AS (each AS event represented by a dot) illustrating the effect sizes (ΔPSI_{betAS}) as the differences between the median group PSIs and their significance assessed by the estimated probability of differential AS, based on the proportion of differences between beta distributed randomly emitted values per sample group that are > 0 ($P_{diff.\ splicing}$). The blue dashed horizontal line indicates the considered cut-off of P_{diff} = 0.95. Points are coloured based on the differential AS calls by both tools: events considered differentially spliced by both `betAS` and `Whippet` (red), by `betAS` (blue) or `Whippet` (purple) alone or by none of the tools (grey). Selected example events are depicted as larger outlined dots. (**B**) `Whippet`'s volcano plot of differential AS illustrating the effect sizes ($\Delta PSI_{Whippet}$) and their significance assessed by `Whippet`'s "probability" (probability that there is some change in ΔPSI, given the read depth of the AS event). The purple dashed horizontal line indicates the considered cut-off of probability = 0.95. Points are coloured based

on the differential AS calls by both tools and selected example events are depicted as larger outlined dots. (**C**) Scatterplot comparing betAS' and Whippet's differential AS significance metrics. betAS' estimated probability of differential AS, based on the proportion of differences between the beta distributed randomly emitted values per group that are > 0 (P_{diff}) and Whippet's probability, with dashed lines defining quadrants indicating the significance cut-offs considered (P_{diff} > 0.95 for betAS, probability > 0.95 for Whippet). Red diagonal solid line indicates identity: $P_{diff\ betAS}$ = $Probability_{Whippet}$. Points are coloured based on the differential AS calls by both tools and selected example events for each quadrant as larger outlined dots. (**D**) Scatterplot comparing betAS' and Whippet's differential AS effect size (ΔPSI). Red diagonal solid line indicates identity: $\Delta PSI_{Whippet}$ = ΔPSI_{betAS}. (**E**) Receiving Operating Characteristic (ROC) curves betAS' differential AS calls with P_{diff} (solid lines) and FPR (dashed lines), considering as ground truth the differential calls from Whippet (dark purple: Probability ≥ 0.9 and |ΔPSI| > 0.1; light purple: Probability > 0.95). (**F** and **G**) Whippet and vast-tools' PSIs (top) and densities of emitted beta distributed values for individual samples (middle) and their merging per sample group (bottom, with dashed lines signing median values) for selected events illustrative of different combinations of effect size and significance of AS differences, identified by vast-tools' IDs (VAST-DB annotation for the mouse mm10 genome assembly): (**F**) MmuEX0013628 (gene *Washc2,* chr6:116256227-116256289), (**G**) MmuEX0053985 (gene *Zmynd8*, chr2:165852868-165852879). ESC: embryonic stem cells.

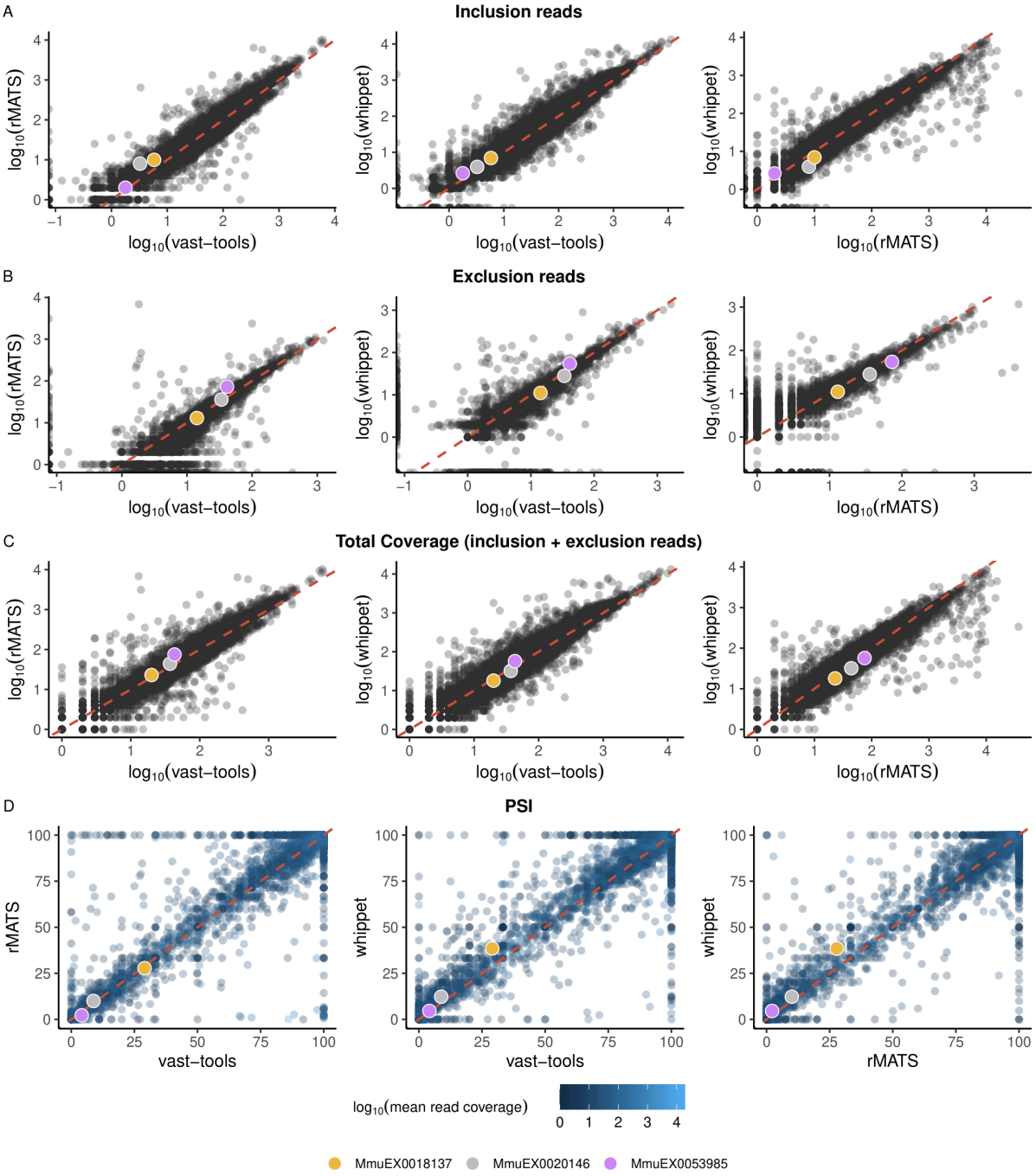

Supplemental Figure S11. Impact of AS tools on event-supporting read counts and PSI values. Scatter plots depicting pairwise comparisons of alternative splicing tools supported by betAS (vast-tools, rMATS, and Whippet) for (**A**) inclusion reads, (**B**) exclusion reads, (**C**) total coverage (sum of inclusion and exclusion reads), and (**D**) Percent Spliced-In (PSI) values within the [0,100] interval. This analysis uses sample SRR645826 from the mouse neuronal differentiation timeline dataset as an example. PSI values (D) are colour-coded based on the mean coverage between the tools being compared. Left plots compare vast-tools with rMATS, middle plots compare vast-tools with Whippet, and right plots compare rMATS with Whippet. Events displayed for each pairwise comparison are those shared between the two tools, identified by their genomic coordinates. Coloured dots highlight three exemplary events discussed in the manuscript.

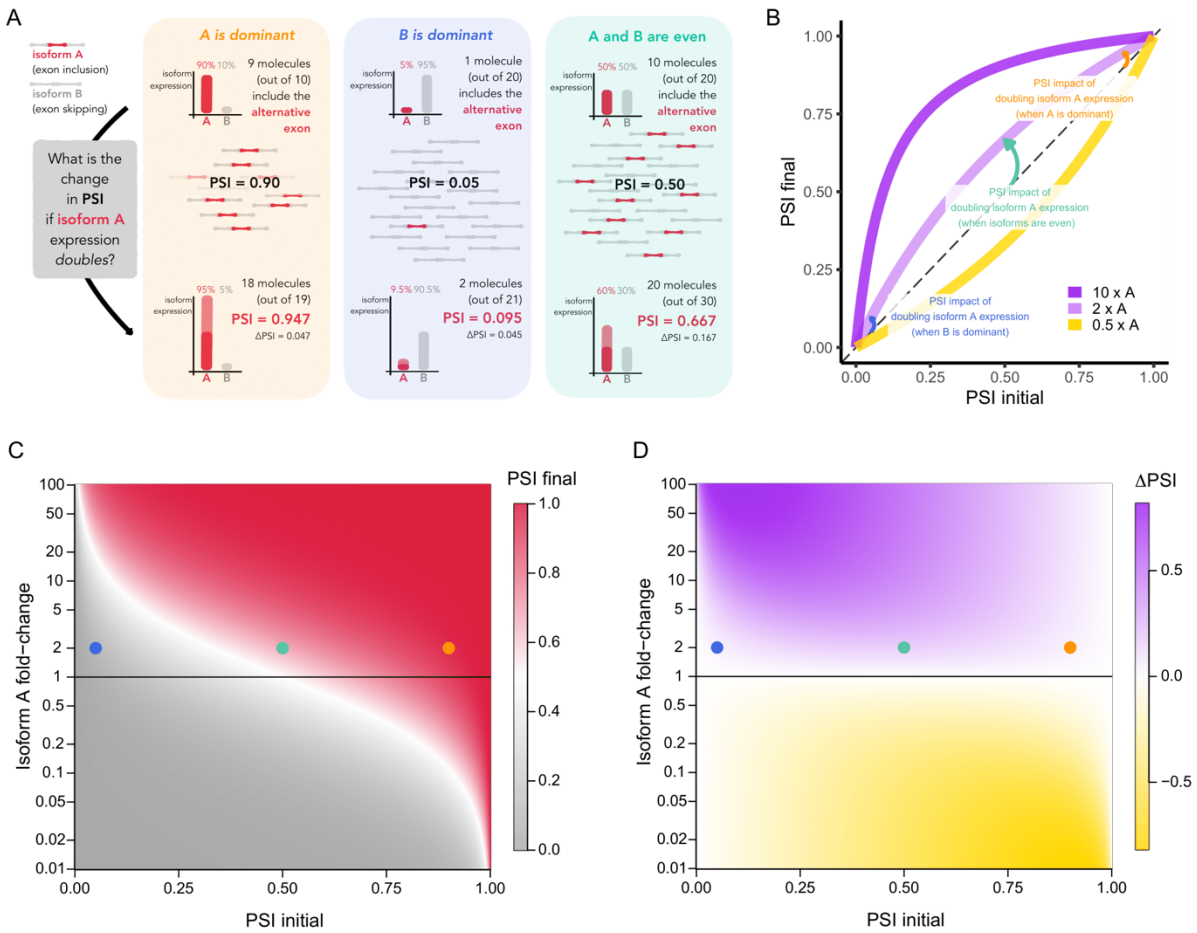

Supplemental Figure S12. The impact of isoform expression changes on the PSI. (**A**) Explanatory diagram illustrative of the impact on the PSI of a duplication in the expression levels of the inclusion isoform in three different scenarios: when A is the dominant isoform (left), when the B isoform is the dominant (middle) and when A and B are evenly distributed. (**B**) Line plots illustrating PSI transitions (i.e., final PSI (Y-axis) against the initial PSI (X-axis)) associated with selected fold-changes of an inclusion isoform. The transitions shown in the three scenarios depicted in panel A are marked as arrows in the respective colours. (**C**) Heatmap showing the continuous spectrum of PSI transitions (i.e. final PSI (heat colour) against the initial PSI (X-axis)) depending on the A isoform fold-change (Y-axis). The transitions shown in the three scenarios depicted in panel A are marked with dots in the respective colours. (**D**) Heatmap showing the continuous spectrum of ΔPSI (final PSI – initial PSI, heat colour) values for PSI transitions depending on the initial PSI (X-axis) and A isoform fold-change (Y-axis). The transitions shown in the three scenarios depicted in panel A are marked with dots in the respective colours.